

# Measurements of thermophysical properties of liquid metals relevant to Marangoni effects

The Royal Society

*Phil. Trans. R. Soc. Lond. A* 1998 **356**, 845-856  
doi: 10.1098/rsta.1998.0191

## Email alerting service

Receive free email alerts when new articles cite this article - sign up in the box at the top right-hand corner of the article or click [here](#)

To subscribe to *Phil. Trans. R. Soc. Lond. A* go to: <http://rsta.royalsocietypublishing.org/subscriptions>

# Measurements of thermophysical properties of liquid metals relevant to Marangoni effects

BY I. EGRY, M. LANGEN AND G. LOHÖFER  
*Institut für Raumsimulation, DLR, 51170 Köln, Germany*

Marangoni convection is caused by a gradient in the surface tension along a free liquid surface. The dimensionless Marangoni number, which controls the strength of this convection, contains additional thermophysical parameters. For liquid metals, these quantities are best measured under containerless conditions using electromagnetic levitation and non-contact diagnostic tools. In microgravity, small electromagnetic fields are sufficient to position a liquid sample. Some experiments can only be performed in such an environment, most others greatly benefit from microgravity and lead to results of higher precision. This paper reports on both terrestrial and microgravity measurements of thermophysical properties of undercooled liquid metals, including specific heat, density, surface tension, viscosity and electrical conductivity.

**Keywords:** oscillating drop technique; electromagnetic levitation; surface tension; density; electrical conductivity; microgravity

## 1. Introduction

Marangoni convection is caused by a gradient in the surface tension  $\gamma$  along a free liquid–vapour interface. This driving force must overcome the resistance of the fluid to flow, characterized by the viscosity  $\eta$ . The dimensionless Marangoni number,  $Ma$ , expresses this competition. It is defined as

$$Ma = (L_s \rho c_p \delta\gamma) / (\lambda \eta), \quad (1.1)$$

where  $L_s$  is a characteristic length,  $\rho$  is the density,  $c_p$  is the specific heat,  $\delta\gamma$  is the difference in surface tension along  $L_s$ , and  $\lambda$  is the thermal conductivity. In order to accurately predict the flow pattern, the thermophysical parameters entering into the definition of the Marangoni number must be precisely known. This is a formidable task, because it involves the measurement of five different parameters. A particular difficulty arises from the determination of  $\delta\gamma$ . In most cases, this difference is due to a temperature gradient  $\delta T$  along  $L_s$ , and it can therefore be written as

$$\delta\gamma = \partial\gamma/\partial T \delta T. \quad (1.2)$$

Therefore, the temperature coefficient of the surface tension has to be determined, which involves the differentiation of the primarily determined surface tension  $\gamma(T)$  with respect to temperature. Accurate results can only be obtained if a wide temperature range is covered and the scatter of the original data points is small.

Inserting equation (1.2) into (1.1), we can separate external quantities from intrinsic material properties by writing

$$Ma = L_s \delta T ma, \quad ma = (\rho c_p \partial\gamma/\partial T) / (\lambda \eta). \quad (1.3)$$

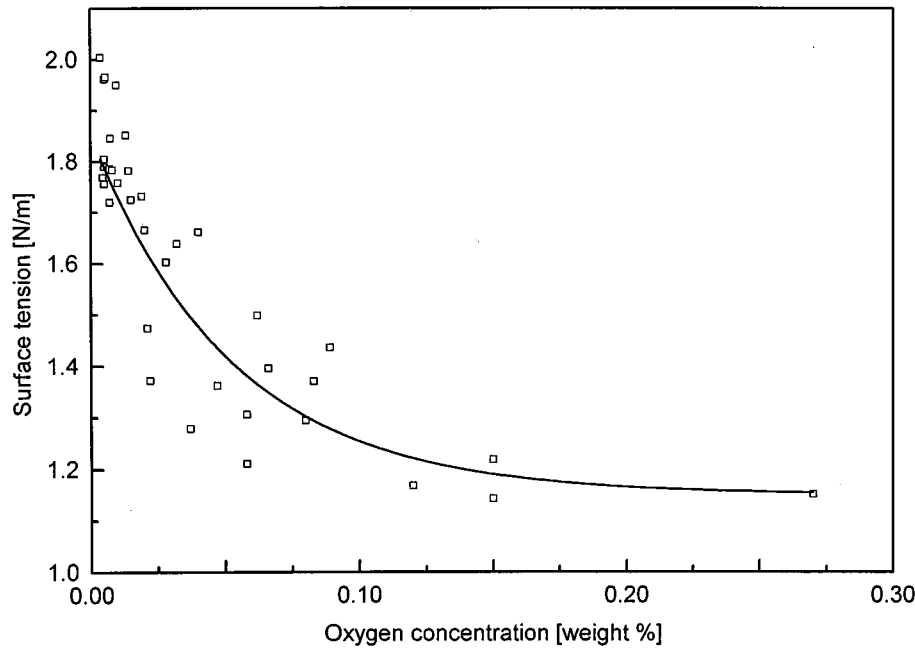


Figure 1. Surface tension of iron as a function of oxygen concentration at 1650 °C (after Keene *et al.* 1982).

We are concerned with the determination of the specific Marangoni number,  $ma$ . Once this quantity is known,  $Ma$  for a given experimental setup can be obtained easily from equation (1.3). Note that  $ma$  can be positive or negative, depending on the sign of  $\partial\gamma/\partial T$ . The temperature coefficient  $\partial\gamma/\partial T$  should be negative for pure elements (with the possible exception of Ga) due to the decrease of structural differences between liquid and gas with increasing temperature; note that, at the critical temperature  $T_c$ , both phases become equal, and, consequently, their interface disappears. However, for alloys, segregation effects may become dominant at low temperatures, leading to a decrease of  $\partial\gamma/\partial T$  with decreasing temperature and thereby to a positive temperature coefficient.

Whereas reliable data exist for fluids which are liquid at, or slightly above, room temperature, the situation is different for high-temperature melts, like liquid metals with a melting temperature around 1000 °C, typically. At these high temperatures ‘everything reacts with everything’ (Mills & Brooks 1994), and it is difficult to find a container that does not contaminate the specimen under investigation. To complicate matters, surface tension is particularly sensitive to even small amounts of impurities. As an example, the surface tension of iron is shown as a function of oxygen concentration in figure 1 (Keene *et al.* 1982).

For liquid metals, electromagnetic levitation provides containerless processing capabilities. An inhomogeneous RF electromagnetic field exerts a Lorentz force on a metallic sample and lifts it against gravity. The ohmic losses of the induced eddy currents in the sample heat, and eventually melt, the sample. If non-contact diagnostic tools can be developed which are compatible with electromagnetic levitation, this combination is best suited for the study of liquid metals. Recently, considerable progress has been made in this direction (Egry *et al.* 1993). Containerless processing has the additional advantage that the liquid metals can be easily undercooled:

due to the absence of container walls, the number of heterogeneous nucleation sites is greatly reduced, and nucleation is delayed. There is, however, one shortcoming of electromagnetic levitation: the electromagnetic fields not only lift and heat the sample, but they also deform its shape and induce potentially turbulent flows in the sample. These undesired side effects cannot be eliminated on Earth and can only partially be accounted for by some extensive magnetohydrodynamic calculations (Cummings & Blackburn 1991; Suryanarayana & Bayazitoglou 1991; Bratz & Egry 1995). For this reason, experiments under microgravity conditions are useful and have been performed (Team TEMPUS 1996).

This paper reviews the non-contact experimental techniques available today in combination with electromagnetic levitation. They allow us to measure all of the thermophysical properties entering the Marangoni number, namely density, specific heat, surface tension, viscosity, and, indirectly, thermal conductivity. A discussion of the results obtained so far, including microgravity experiments, is also included.

## 2. Specific heat

The specific heat  $c_p$  describes the temperature change of a body due to heat input or heat loss:

$$mc_p \frac{dT}{dt} = P_{\text{in}} - P_{\text{out}}, \quad (2.1)$$

where  $m$  is the mass of the body and  $P_{\text{in}}$  and  $P_{\text{out}}$  are the power input and output, respectively. In electromagnetic levitation, power is fed into the sample by induction. The power absorbed by the sample is proportional to the power drawn by the levitation coil. Once this coupling coefficient is known, the power absorbed by the sample can be calculated from the power draw of the RF circuit. To determine the specific heat, the heat loss must also be known. This is most easily achieved in vacuum conditions, where there are only radiative heat losses:

$$P_{\text{out}} = \sigma_{\text{SB}} A \epsilon T^4, \quad (2.2)$$

where  $\sigma_{\text{SB}}$  is the Stefan–Boltzmann constant,  $A$  is the surface area of the specimen, and  $\epsilon$  is the total hemispherical emissivity. In terrestrial levitation, convective cooling is always required to control and limit the sample temperature. The effect of the cooling gas has to be taken into account in the heat balance (equation (2.1)), and, if convection is present, the heat loss to the gas cannot be simply described by an effective thermal conductivity. Therefore, the applicability of this method is limited to microgravity experiments.

If the total hemispherical emissivity is known, the specific heat can be obtained from cooling curves, i.e.  $P_{\text{in}} = 0$ . In such a case,  $c_p$  is simply given by

$$c_p = - \frac{\sigma_{\text{SB}} A \epsilon}{m} \frac{T^4}{dT/dt}. \quad (2.3)$$

Unfortunately, in most cases,  $\epsilon$  is not known. Nevertheless, the specific heat can be determined through a modulation technique, developed by Fecht & Johnson (1991). The heater power is modulated according to  $P(t) = P_\omega \cos(\omega t)$  resulting in a modulated temperature response  $\Delta T_\omega$  of the sample. Temperature gradients inside the sample relax quickly, due to the high thermal conductivity of metals. This relaxation can be described by a relaxation time  $\tau_{\text{int}}$ . On the other hand, relaxation to the equilibrium temperature is governed by radiation under UHV conditions, and is therefore

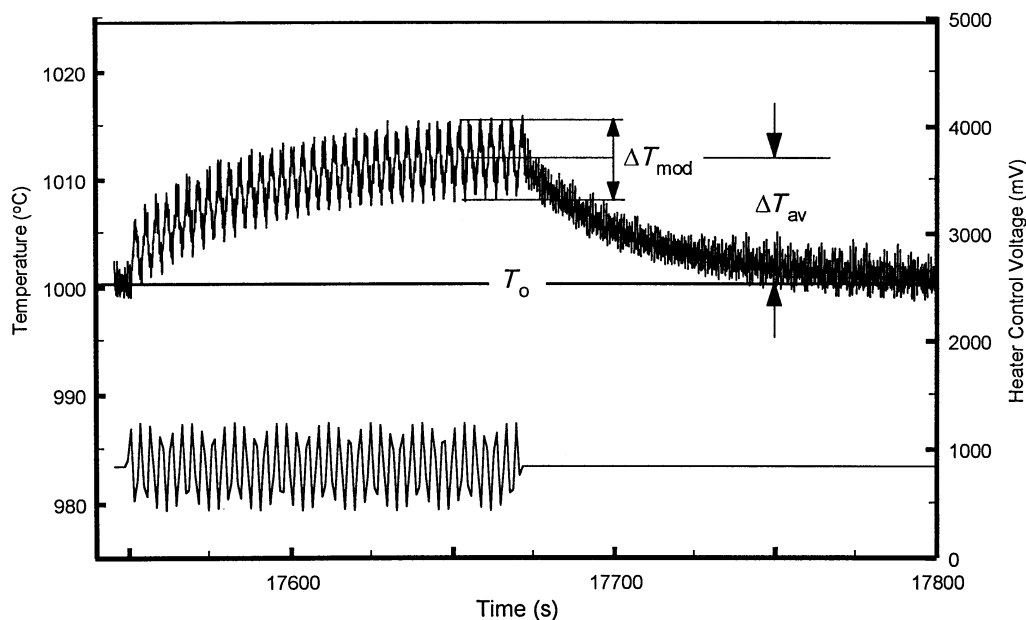


Figure 2. AC calorimetry on ZrNi alloy: power modulation and temperature response

slow. It can be described by a relaxation time  $\tau_{\text{ext}}$ . If the modulation frequency  $\omega$  is chosen such that  $1/\tau_{\text{ext}} \ll \omega \ll 1/\tau_{\text{int}}$ , a simple relation for the temperature variation can be derived:

$$\Delta T_{\omega} = P_{\omega}/(\omega c_p), \quad (2.4)$$

from which  $c_p$  can be determined.

In practice, the power input into the sample is controlled by a control voltage  $U_c$ :

$$P_{\text{in}} = \alpha U_c^2, \quad (2.5)$$

where  $\alpha$  is a constant characterizing the RF circuit including the sample. The control voltage is modulated according to

$$U_c = U_0 + U_m \cos(\omega t), \quad (2.6)$$

resulting in a power modulation at the sample:

$$P_{\text{in}} = \alpha(U_0^2 + \frac{1}{2}U_m^2 + 2U_0U_m \cos(\omega t) + \frac{1}{2}U_m^2 \cos(2\omega t)). \quad (2.7)$$

The first term is the unmodulated RF power. It determines the equilibrium temperature of the sample before modulation. As we can see from (2.7), the modulation produces a periodic temperature response (third and fourth terms) superimposed over an increase in the average sample temperature (second term). Equation (2.4) can be applied to the third and fourth term separately. Figure 2 shows data taken from an  $\text{Ni}_{24}\text{Zr}_{76}$  sample flown on IML-2 (Team TEMPUS 1996) with the corresponding heater control voltage plotted below.

Of course, specific heat data from liquid, and even undercooled metals, can also be measured using drop calorimeters (Barth *et al.* 1993). The fundamental problem of drop calorimetry is due to the fact that the specific heat is not measured directly, but is obtained by differentiating the measured enthalpy with respect to temperature. To discuss these measurements in any detail is outside the scope of the present article.

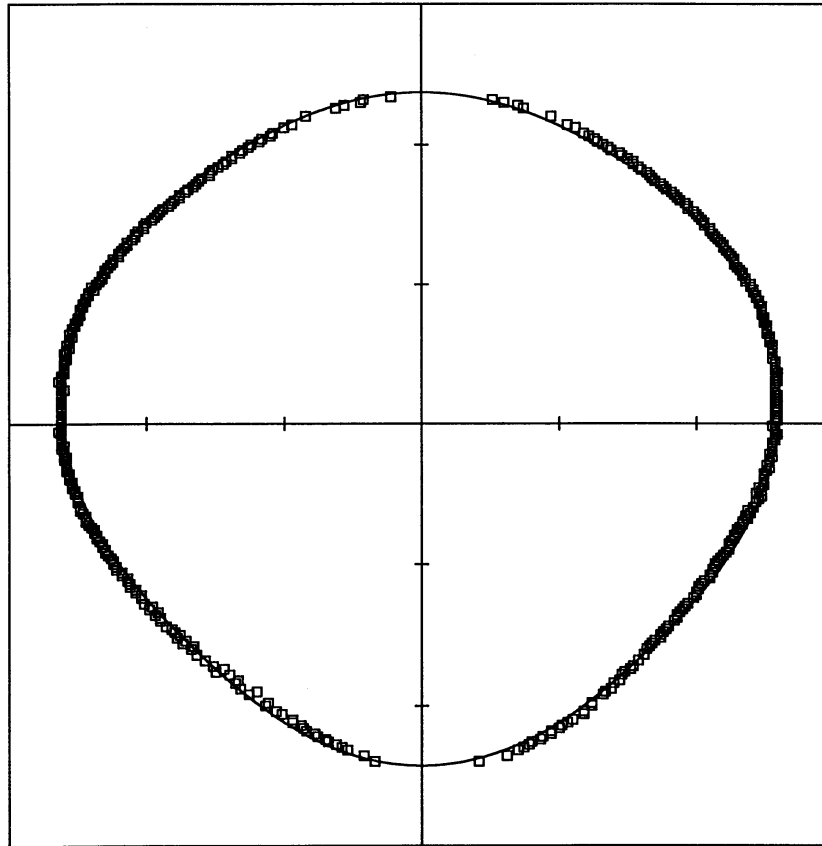


Figure 3. Shape of a levitated silicon sample and fit with Legendre polynomials.

### 3. Density

Density measurements of levitated samples can be made using videography. In terrestrial levitation, samples are not spherical, but slightly elongated due to the action of gravity and the electromagnetic field. However, their static equilibrium shape is still rotationally symmetrical around the vertical axis (parallel to the gravity vector). Therefore, images are taken perpendicular to this axis, and the volume  $V$  of a rotationally symmetrical body is calculated. The mass  $m$  of the sample is known; it is weighed before and after the measurement. The density of the sample is then obtained from

$$\rho = m/V. \quad (3.1)$$

The images are taken at constant temperature and analysed off-line by a digital image processing system. In a first step, the software detects the edge of the incandescent sample; then an average of approximately 100 images is performed to remove the potentially asymmetrical dynamic surface oscillations. Finally, the shape of the averaged image is fitted with a series of Legendre polynomials.

An example of such a fit is shown in figure 3.

Once the coefficients of this series expansion are known, the volume and hence the density can be calculated. A detailed description of this algorithm has been given in

*Phil. Trans. R. Soc. Lond. A* (1998)

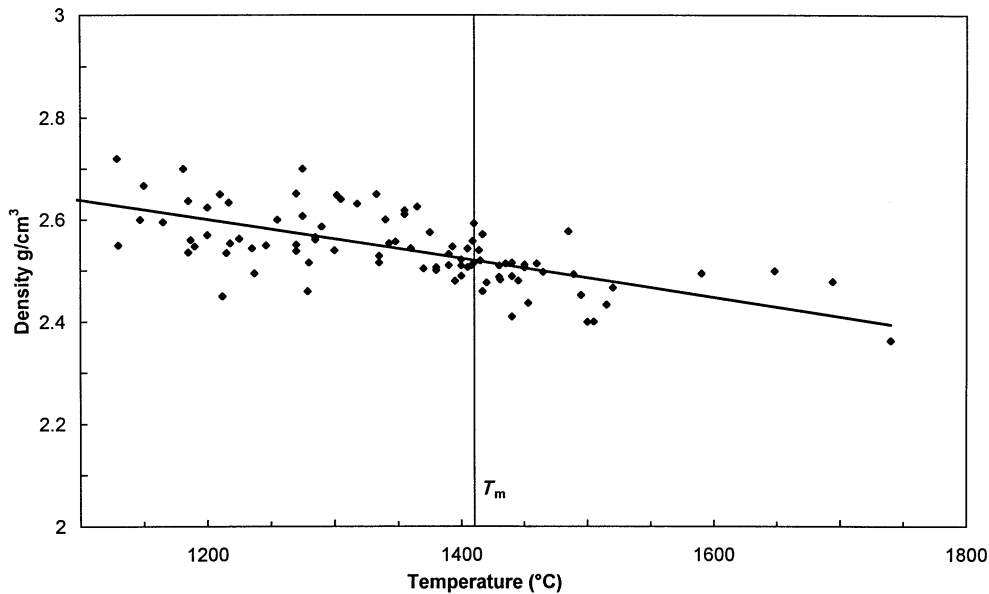


Figure 4. Density of liquid silicon as function of temperature.

Gorges *et al.* (1996). Using this method, we have recently determined the density of liquid silicon over a wide temperature range. The result is shown in figure 4.

This example shows that it is even possible to apply electromagnetic levitation to semiconductors.

#### 4. Surface tension and viscosity

##### (a) Surface tension

The oscillating drop technique is an elegant way to measure both surface tension and viscosity. It employs digital image processing for frequency analysis of surface waves. The radius  $a$  of a droplet undergoes oscillations of the form

$$\delta a_{l,m}(\vartheta, \phi, t) \propto Y_{l,m}(\vartheta, \phi) \cos(\omega_{l,m}t) e^{-\Gamma_{l,m}t}. \quad (4.1)$$

Here,  $Y_{l,m}$  are spherical harmonics. The frequency  $\omega_{l,m}$  is related to surface tension, while the damping  $\Gamma_{l,m}$  of the waves is due to viscosity. If the equilibrium shape of the droplet is spherical, the simple formulae of Rayleigh and Kelvin can be used to relate frequency  $\omega$  and damping  $\Gamma$  of the oscillations to surface tension  $\gamma$  and viscosity  $\eta$ , respectively. Rayleigh's formula reads

$$\omega_R^2 = \frac{32}{3} \pi (\gamma/m), \quad (4.2)$$

while Kelvin derived the following expression:

$$\Gamma_K = \frac{20}{3} \pi (a\eta/m), \quad (4.3)$$

where  $m$  is the mass of the droplet and  $a$  is its radius. These two expressions relate to the fundamental mode of oscillation, which corresponds to  $l = 2$ . For spherical drops, frequencies and damping constants do not depend on  $m$  ( $|m| < 2$ ). A spherical shape is obtained only if the droplet is free of external forces. This situation is well approximated in microgravity. Under terrestrial conditions, the above relations are

Table 1. Surface tension of liquid transition and noble metals

element	$\gamma_m$ (mN m <sup>-1</sup> )		$\gamma_T$ (mN m <sup>-1</sup> K <sup>-1</sup> )	
	this work	Keene	this work	Keene
Fe	1870	1862	0.43	0.39
Co	1874	1881	0.3	0.34
Ni	1770	1796	0.33	0.35
Cu	1304	1330	0.22	0.23
Ag	908	925	0.18	0.21
Au	1149	1145	0.14	0.18

not valid and corrections have to be made for the external forces, namely gravity and electromagnetic field. These corrections have been calculated recently (Cummings & Blackburn 1991; Suryanarayana & Bayazitoglou 1991; Bratz & Egry 1995). They take into account both the splitting of the peaks due to symmetry breaking, and the shifting of the peaks due to magnetic pressure. For the Rayleigh formula the correction reads

$$\frac{32}{3}\pi(\gamma/m) = \frac{1}{5} \sum_m \omega_{2,m}^2 - 1.9\overline{\Omega_{tr}^2} - 0.3(\overline{\Omega_{tr}^2})^{-4}(g/a)^2 \quad (4.4)$$

Here,  $\overline{\Omega_{tr}^2}$  is the mean of the translational frequencies of the sample in the potential well of the levitation field, and  $g$  is the gravitational acceleration. It has been shown that by applying the Cummings correction to surface tension data obtained by the oscillating drop technique on Earth, a spurious mass dependence can be eliminated (Egry 1994). For gold, the value thus obtained agrees well with data obtained using the sessile drop technique. In addition, Egry and coworkers have performed microgravity experiments on gold and a gold–copper alloy (Egry *et al.* 1995). These experiments clearly show a single peak in the oscillation spectrum which means that the frequencies do not depend on  $m$  and, furthermore, they yield values for the surface tension which are in excellent agreement with terrestrial data only if the latter are corrected according to equation (4.4).

Using the oscillating drop method and applying the Cummings correction, we have measured the surface tension of a number of liquid metals. The temperature dependence of the surface tension of pure elements is conveniently described by

$$\gamma(T) = \gamma_m - \gamma_T(T - T_m), \quad (4.5)$$

where  $T_m$  is the melting temperature. Our results for noble and transition metals are listed in table 1. For comparison, the recommended values of Keene (1993) are also shown. Generally speaking, the agreement is excellent, with our data being somewhat lower. This may be due to the fact that Keene's compilation also contains data obtained with the oscillating drop technique, but without Cummings correction.

So far, we have only discussed pure elements. In the case of alloys, the surface tension depends on both temperature and concentration. Whereas the temperature dependence is essentially linear, the concentration dependence is more complicated. This is due to surface segregation effects. In alloys, the system uses its additional degree of freedom to minimize its free energy. It can do so by segregating the



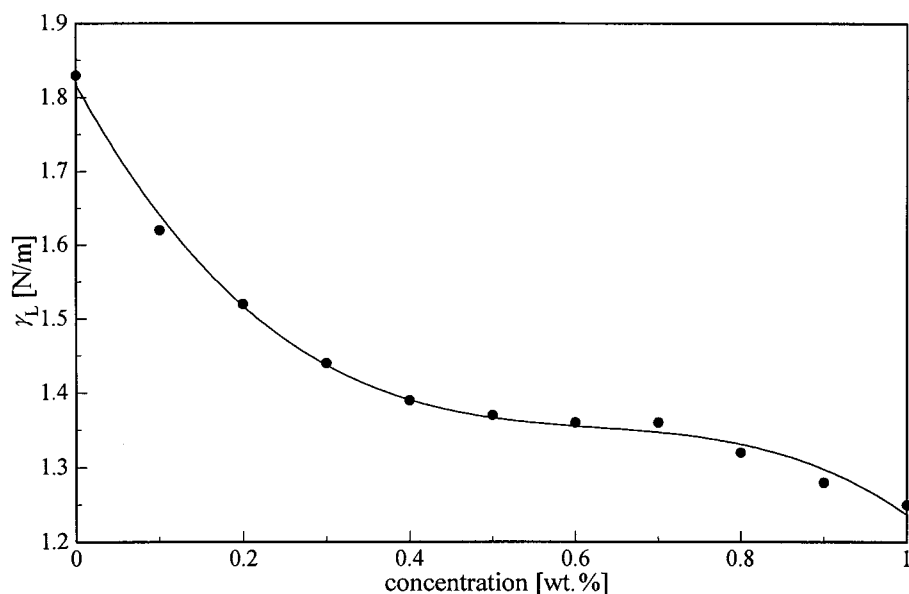


Figure 5. Surface tension of the system Cu–Ni.

component with lower surface tension at the surface. This gain in energy is partly compensated by loss of entropy, particularly at high temperatures. The surface tension of alloys can be calculated from conventional bulk thermodynamics if the mixing character is known. For the simplest case of an ideal solution, the following explicit formula can be given:

$$\gamma_{\text{mix}} = \gamma_1 - \tilde{\gamma} \ln\{c_1 + (1 - c_1) \exp(\Delta\gamma/\tilde{\gamma})\}, \quad (4.6)$$

where  $\gamma_1$  and  $c_1$  are the surface tension and concentration of component 1, respectively. The difference between the surface tensions of the pure components is  $\Delta\gamma = \gamma_1 - \gamma_2$ , and  $\tilde{\gamma} = RT/f$ , where  $f$  is the surface area of one mole of either species. Usually  $f$  is treated as a fitting parameter. More generally, the surface tension of alloys is calculated from Butler's formula assuming either regular or subregular solutions (Hajra *et al.* 1991). We have measured the surface tension of the simple system Cu–Ni (Gorges 1996). It is a completely miscible system with a very simple phase diagram. Therefore, one should expect ideal mixing behaviour. However, as can be seen from figure 5, CuNi does not mix ideally, and it is best described by a regular solution model.

#### (b) Viscosity

In the case of viscosity, the Kelvin formula (equation (4.3)) is derived for force-free samples under the assumption of purely laminar flow. Whereas the effect of external forces on the equilibrium shape can be taken into account (as long as they can be treated as a small perturbation), this is certainly not true when they cause turbulent flow. In such a case, turbulence introduces additional damping which masks the damping due to viscosity. This seems to be the case for both terrestrial and microgravity electromagnetic levitation. Therefore, until now, no viscosity data could be derived from the oscillating drop technique. If the levitation fields can be further reduced, there is hope that this method can be applied to high-viscosity systems such as PdCuSi or the recently discovered easy glass formers (Johnson 1996; Inoue

*et al.* 1994). Corresponding microgravity experiments are under way: a reflight of the TEMPUS facility is planned for SpaceHab mission MSL-1 in July 1997. Conventional methods like the oscillating vessel or oscillating bob viscometers are difficult to use for liquid metals and can have errors of up to 50% (Iida & Guthrie 1993). One way of at least estimating viscosity values in the liquid and undercooled regime is provided by the simple formula (Egry 1993):

$$\gamma/\eta = \frac{15}{16} \sqrt{kT/m}. \quad (4.7)$$

## 5. Conductivity

Finally, it is also possible to measure the electrical conductivity  $\sigma$  of levitated droplets. This can be done using non-contact inductive methods. The basic idea is to place a pickup coil around the sample and to measure the impedance  $Z$  of the system (Lohöfer 1994). Being a complex quantity,  $Z$  contains information about the ratio of the amplitudes of voltage and current,  $U_0/I_0$ , as well as their phase shift  $\phi$ . Any changes in the impedance can be attributed to changes of the sample. Two effects can influence the impedance, namely the sample can either change its conductivity or its shape. For conductivity measurements it is essential that these two effects can be separated. It can be shown that for small skin depth  $\delta$  and small deviations from a spherical shape, this is indeed the case, if the pickup coil has a special geometry. The skin depth  $\delta$  is defined as

$$\delta = \sqrt{2/\omega\mu_0\sigma}. \quad (5.1)$$

Here,  $\omega$  is the oscillation frequency of the generator circuit,  $\mu_0$  is the magnetic permeability and  $\sigma$  is the conductivity. Therefore, small skin depth implies high frequency or high conductivity. In terrestrial levitation experiments, the levitation coil cannot be used as a pickup coil for impedance measurements and an additional measuring coil has to be introduced. In microgravity experiments, the heating coil has the required symmetry and can be used as pickup coil. In addition, the liquid sample is spherical. For such a geometry, a simple relation can be derived between  $U_0/I_0$  and  $\delta$ , which allows the determination of the conductivity. It reads

$$\delta = \frac{a}{2} \left( 1 - \sqrt{1 - 4 \left\{ \frac{A}{U_0/I_0} - B \right\}} \right). \quad (5.2)$$

$A$  and  $B$  are two constants characterizing the empty coil and  $a$  is the radius of the sample. During the SpaceHab mission IML-2, the electrical conductivity of a  $\text{Zr}_{64}\text{Ni}_{36}$  alloy was measured in the TEMPUS facility using the approach outlined above. Figure 6 shows the result.

Presently, we are developing modified coil systems and an improved theory which will allow us to measure the electrical conductivity of slightly deformed samples on Earth.

To obtain the thermal conductivity  $\lambda$ , needed to complete the definition of the specific Marangoni number  $ma$ , we have to use the Wiedemann–Franz law which relates thermal and electrical conductivity (Iida & Guthrie 1993):

$$\lambda/\sigma = LT, \quad (5.3)$$

where  $L$  is the Lorenz number:  $L = 2.45 \times 10^8 \text{ V}^2 \text{ K}^{-2}$ . The Wiedemann–Franz law is known to hold well for metals at high temperatures.

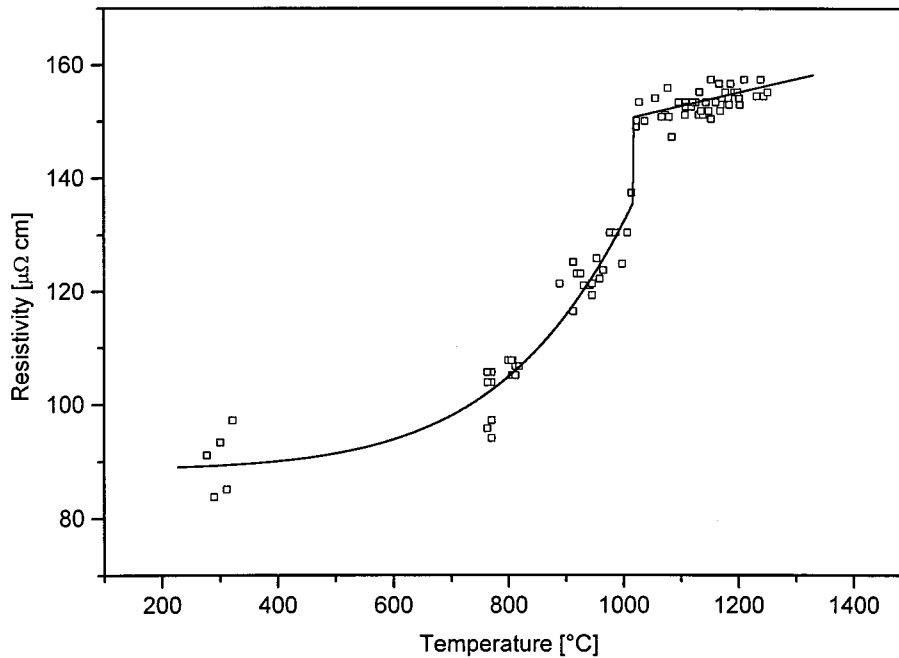


Figure 6. Electrical resistivity of  $Zr_{64}Ni_{36}$  in the solid and liquid phase.

## 6. Conclusion

The measurement of all thermophysical properties determining the Marangoni number is a difficult task, in particular for liquid metals at high temperatures. A promising strategy is to use containerless methods which avoid contamination of the sample. Non-contact diagnostic tools are available or are being developed. With their help, the database on thermophysical properties of liquid metals will be expanded and consolidated. Some of the presented experiments rely on a microgravity environment and can therefore not yet be performed routinely. With the advent of a permanent space station, frequent experimental campaigns should become possible improving the accuracy and fidelity of the data.

## References

- Barth, M., Joo, F., Wei, B. & Herlach, D. M. 1993 *J. Non-crystal. Solids* **156–158**, 398.  
 Bratz, A. & Egry, I. 1995 *J. Fluid Mech.* **298**, 341.  
 Cummings, D. & Blackburn, D. 1991 *J. Fluid Mech.* **224**, 395.  
 Egry, I. 1993 *Scripta Metal. Mater.* **28**, 1273.  
 Egry, I. 1994 *Mat. Sci. Engng A* **178**, 73.  
 Egry, I., Lohöfer, G. & Sauerland, S. 1993 *Int. J. Thermophys.* **14**, 573.  
 Egry, I., Lohöfer, G. & Jacobs, G. 1995 *Phys. Rev. Lett.* **75**, 4043.  
 Fecht, H. & Johnson, W. 1991 *Rev. Sci. Instrum.* **62**, 1299.  
 Gorges, E. 1996 Ph.D. thesis, University of Aachen.  
 Gorges, E., Racz, L. M., Schillings, A. & Egry, I. 1996 *Int. J. Thermophys.* **17**, 1163.  
 Hajra, J. P., Lee, H.-K. & Froberg, M. G. 1991 *Z. Metal.* **82**, 603.  
 Iida, T. & Guthrie, R. I. L. 1993 *The physical properties of liquid metals*. Oxford: Clarendon.  
 Inoue, A., Kawase, D., Tsai, A. P., Zhang, T. & Masumoto, T. 1994 *Mat. Sci. Engng A* **178**, 255.

- Johnson, W. L. 1996 *Materials science forum*, vol. 35, pp. 225–227. Switzerland: Transtech Publications.
- Keene, B. J. 1993 *Int. Mat. Rev.* **38**, 157.
- Keene, B. J., Mills, K. C., Bryant, J. W. & Hondros, E. D. 1982 *Can. Met. Q.* **21**, 393.
- Lohöfer, G. 1994 *Int. J. Engng Sci.* **32**, 107.
- Mills, K. C. & Brooks, R. F. 1994 *Mat. Sci. Engng A* **178**, 77.
- Suryanarayana, P. V. R. & Bayazitoglou, Y. 1991 *Phys. Fluids A* **3**, 967.
- Team TEMPUS 1996 *Materials and fluids under low gravity* (ed. L. Ratke, H. Walter & B. Feuerbacher), p. 233. Berlin: Springer.

### Discussion

J. C. EARNSHAW (*Department of Pure and Applied Physics, University of Belfast, UK*). The elegant and non-invasive methods outlined in this paper promise very clean data on thermophysical properties of liquid metals. I am, however, somewhat concerned about certain effects which may influence the values of viscosity determined from the damping of the oscillations of a liquid metal drop.

Simulations have suggested that density oscillations exist at the surface of a liquid metal, reflecting the variation of the conduction electron density through the transition zone (D'Evelyn & Rice 1981). Such a layered structure at a liquid metal–vapour interface, extending some few atomic layers into the bulk, has been confirmed by X-ray reflectivity studies (Sluis & Rice 1983; Magnussen *et al.* 1995). Such a structure could act as an interfacial molecular film, supporting dilatational surface waves. Such dilatational modes would couple to the capillary modes Dr Egly observed; the main effect would be to increase the damping of the capillary modes (Lucassen-Reynders & Lucassen 1969; Kramer 1971). Indeed light scattering studies of thermally excited capillary waves on the clean surface of Hg show such increased damping (Kolevson, personal communication). The expected effects are shown in figure 7 for capillary waves of wave number  $q = 10 \text{ cm}^{-1}$  (comparable to those in experiments by Dr Egly) on a planar Hg–vacuum interface. The considerable increase in the wave damping for non-zero dilatational elastic moduli is apparent. While the theoretical formulation is more complex for oscillations of spherical droplets (Sparling & Sedlak 1989) the two surface modes couple similarly in this case also, again leading to increased capillary mode damping. This suggests that viscosities deduced from the observed damping values might be significantly and systematically overestimated. The changes in the capillary mode frequency are orders of magnitude less than those in the damping (see figure 7), so that estimates of surface tension should be relatively unaffected.

I. EGRY. Professor Earnshaw makes a very important remark about the interpretation of the damping of capillary waves. He points out that the damping may be due to other mechanisms than viscosity, in particular coupling to dilatational surface waves may lead to damping of the capillary waves. Strong damping of thermally excited capillary waves observed on a clean planar surface of liquid Hg was interpreted as being due to such an effect, assuming that such a surface layer is an intrinsic property of a liquid metal and would exist even on clean surfaces.

In the experiments discussed in our paper, the damping of mechanically excited oscillations of a liquid drop is observed. If surface dilatational waves existed on the surface, it is very likely that a similar mode-coupling as in the planar case would lead to an enhanced damping. However, this is not the case experimentally. Recently, we have evaluated our microgravity experiment on the eutectic Pd<sub>78</sub>Cu<sub>6</sub>Si<sub>16</sub> alloy, using

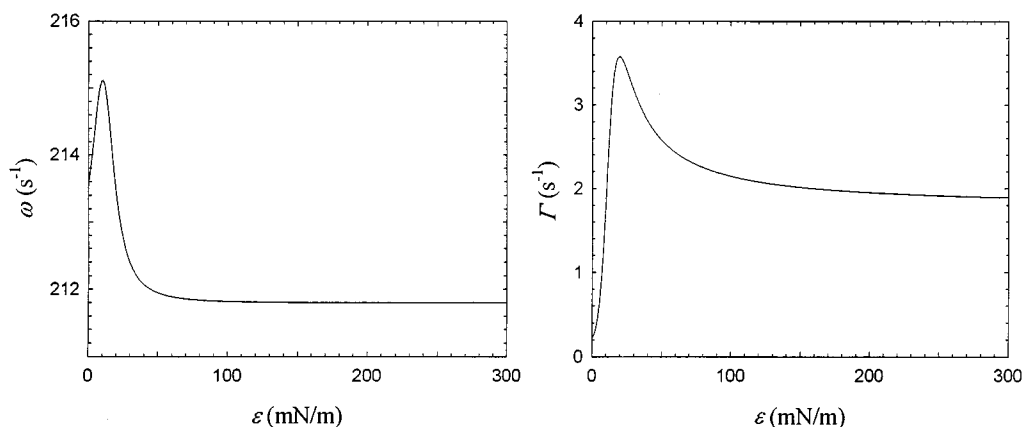


Figure 7. The capillary wave frequency ( $\omega$ ) and damping ( $\Gamma$ ) for capillary waves of  $q = 10 \text{ cm}^{-1}$  on a Hg–vacuum interface as a function of the dilatational elastic modulus  $\varepsilon$ . The damping varies by a factor of over 10, whereas the variations of the frequency are less than 0.7% of the value for  $\varepsilon = 0$ .

the simple formula  $\Gamma = \frac{20}{3}\pi(a\eta/m)$  (equation (4.3) of our paper), which assumes damping by viscosity only. For the viscosity at the eutectic temperature  $T = 760^\circ\text{C}$ , our preliminary analysis yields  $\eta = 49 \text{ mPa s}$  (Egry *et al.* 1998). Previously, the viscosity of  $\text{Pd}_{78}\text{Cu}_6\text{Si}_{16}$  was measured by Lee *et al.* (1991). They obtained  $\eta = 61 \text{ mPa s}$  at the same temperature. Our value is of the same order of magnitude, but lower than theirs. An additional damping due to the coupling to surface dilatational waves, seems therefore negligible. More work, both theoretical and experimental, is needed to clarify this puzzle.

#### Additional references

- Egry, I., Lohöfer, G., Seyhan, I. & Schneider, S. 1998 (In the press.)  
 D'Evelyn, M. P. & Rice, S. A. 1981 *Faraday Symp. Chem. Soc.* **16**, 71.  
 Kramer, L. 1971 *J. Chem. Phys.* **55**, 2097.  
 Lee, S. K., Tsang, K. H. & Kui, H. W. 1991 *J. Appl. Phys.* **79**, 4842.  
 Lucassen-Reynders, E. H. & Lucassen, J. 1969 *Adv. Colloid. Interf. Sci.* **2**, 347.  
 Magnussen, O. M., Ocko, B. M., Regan, M. J., Penanen, K., Pershan, P. S. & Deutsch, M. 1995 *Phys. Rev. Lett.* **74**, 4444.  
 Sluis, D. & Rice, S. A. 1983 *J. Chem. Phys.* **79**, 5658.  
 Sparling, L. C. & Sedlak, J. E. 1989 *Phys. Rev. A* **39**, 1351.